Simulation of Dense Colloids

H. J. Herrmann
Computational Physics, IfB, Schafmattstr. 6, ETH Zürich, CH-8093 Zürich, Switzerland and
Departamento de Física, Universidade Federal do Ceará, 60451-970 Fortaleza, CE, Brazil

J. Harting and M. Hecht
Institute for Computational Physics, Pfaffenwaldring 27, 70569 Stuttgart, Germany

E. Ben-Naim
Theoretical Division and Center for Nonlinear Studies,
Los Alamos National Laboratory, Los Alamos, New Mexico 87545, USA

Received on 31 August, 2007

We present in this proceeding recent large scale simulations of dense colloids. On one hand we simulate model clay consisting of nanometric aluminum oxyde spheres in water using realistic effective electrostatic interactions and Van der Waals attractions, known as DLVO potentials and a combination of molecular dynamics (MD) and stochastic rotation dynamics (SRD). We find pronounced cluster formation and retrieve the shear softening of the viscosity in quantitative agreement with experiments. On the other hand we study the velocity probability distribution functions (PDF) of sheared hard-sphere colloids using a combination of MD with lattice Boltzmann and find strong deviations from a Maxwell-Boltzmann distribution. We find a Gaussian core and an exponential tail over more than six orders of magnitude of probability. The simulation data follow very well a simple theory. We show that the PDFs scale with shear rate $\dot{\gamma}$ as well as particle volume concentration ϕ, and kinematic viscosity ν.

Keywords: Computer simulations; Molecular Dynamics; SRD, Lattice Boltzmann; Colloids; Shear cell; Rheology

I. INTRODUCTION

Colloids are ubiquitous in our daily life including coffee, tooth paste and wall paint which are mixtures of finely ground solid ingredients in a fluid. Of particular interest for industrial applications are suspensions under the influence of external forces causing sedimentation or shear flows. Detailed experiments have been performed for more than a hundred years, but questions about the microstructure during sedimentation or structural relaxations of the sediment are still not well understood. Colloids behave in a complex way, since different time and length scales are involved. The particle sizes are on a mesoscopic length scale, i.e., in the range of nanometers up to micrometers. Depending on the particle sizes, materials, and concentrations, different interactions are of relevance and often several of them are in a subtle interplay: electrostatic repulsion, depletion forces, van der Waals attraction, hydrodynamic interaction, Brownian motion, and gravity are the most important influences. Here, we are interested in colloids, where attractive van der Waals interaction is important for the description, i.e., where under certain circumstances cluster formation plays an important role[1, 2]. To model these systems experimentally, Al_2O_3 suspensions are often used[3, 4]. Al_2O_3 is also a common material in the ceramics industry. There, wet processing of suspensions, followed by a sinter process is a common practice. The stability of the resulting workpiece strongly depends on the microstructure formed before the sintering process. The viscosity, velocity distribution and stability of clusters as well as their formation are only a few of the quantities of interest. We will present large scale simulations and study in particular the anomalous velocity distribution under shear.

II. SIMULATING SHEARED CLAY

We investigate the rheology of a sheared solution of spherical Al_2O_3 particles of diameter $0.37\,\mu$m in water. Clusters of particles can form for two different reasons: depletion forces[5, 6], like-charge attraction mediated by the counterions in the solvent[7, 8], or van der Waals attraction[9–11]. The shear flow can either support cluster formation at low shear rates, or it can suppress cluster formation at high shear rates as we have shown in ref. [12]. We adjust the simulation parameters so that the simulation corresponds quantitatively to a real suspension with 35% volume concentration under shear. The shear rate is kept fixed at $\dot{\gamma} = 20/s$[13, 14]. For Al_2O_3 suspensions attractive van der Waals forces compete with electrostatic repulsion. Depending on the particle surface charge, clustering due to attractive van der Waals forces can dominate or be prevented. We have presented how one can relate parameters of DLVO potentials[15, 16] with experimentally tunable parameters, i.e., the pH-value and the salt concentration expressed by the ionic strength I, influence the charge of the colloidal particles[14]. We explored the stability diagram of Al_2O_3 suspensions and reproduced that the particles are uncharged close to the so called "isoelectric point" at pH = 8.7, where they form clusters regardless of the ionic strength. For lower pH-values particles can be stabilized in solution. For very low pH-values, low salt concentrations, and high volume fractions a repulsive structure can be found. The particle size is on a mesoscopic length scale, where Brownian motion is relevant and long range hydrodynamic interactions

are of importance. Therefore, we use "Stochastic Rotation Dynamics" (SRD), which includes both, hydrodynamics and Brownian motion for the description of the fluid [17, 18].

Our simulation method is described in detail in ref. [13, 14] and consists of two parts: a Molecular Dynamics (MD) code, which treats the colloidal particles, and a Stochastic Rotation Dynamics (SRD) simulation for the fluid solvent. In the MD part we include effective electrostatic interactions and van der Waals attraction, known as DLVO potentials[15, 16], a lubrication force and Hertzian contact forces. DLVO potentials are composed of two terms, the first one being an exponentially screened Coulomb potential due to the surface charge of the suspended particles

$$V_{\mathrm{Coul}} = \pi\varepsilon_r\varepsilon_0 \left[\frac{2+\kappa d}{1+\kappa d}\cdot\frac{4k_{\mathrm{B}}T}{ze}\tanh\left(\frac{ze\zeta}{4k_{\mathrm{B}}T}\right)\right]^2 \times\frac{d^2}{r}\exp(-\kappa[r-d]). \quad (1)$$

Here d denotes the particle diameter, r the distance between the particle centers, e the elementary charge, T the temperature, k_{B} the Boltzmann constant, and z is the valence of the ions of added salt. ε_0 is the permittivity of the vacuum, $\varepsilon_r = 81$ the relative dielectric constant of the solvent, κ the inverse Debye length defined by $\kappa^2 = 8\pi\ell_B I$, with ionic strength I and Bjerrum length $\ell_B = 7\mathring{A}$. The first fraction in eq.(1) is a correction to the DLVO potential (in the form used in ref. [9]), which takes the surface curvature into account and is valid for spherical particles. The effective surface potential ζ can be related to the pH-value of the solvent with a $2pK$ charge regulation model[14]. The Coulomb term competes with the attractive van der Waals interaction ($A_{\mathrm{H}} = 4.76\cdot 10^{-20}$ J is the Hamaker constant)[9]

$$V_{\mathrm{VdW}} = -\frac{A_{\mathrm{H}}}{12}\left[\frac{d^2}{r^2-d^2}+\frac{d^2}{r^2}+2\ln\left(\frac{r^2-d^2}{r^2}\right)\right]. \quad (2)$$

The attractive contribution V_{VdW} is responsible for cluster formation. However, depending on the pH-value and the ionic strength, it may be overcompensated by the electrostatic repulsion. When particles get in contact, the potential has a minimum. However, eq.(2) diverges due to the limitations of DLVO theory. We cut off the DLVO potentials and model the minimum by a parabola. The particle contacts are modeled as Hertzian contacts and for non-touching particles, below the resolution of the SRD algorithm short range hydrodynamics is corrected by a lubrication force, which we apply within the MD framework, as we have explained in ref. [13, 14]. For the integration of translational motion of the colloidal particles we use a velocity Verlet algorithm[19] and for the fluid we apply the Stochastic Rotation Dynamics method (SRD)[17, 18]. It intrinsically contains fluctuations, is easy to implement, and has been shown to be suitable for simulations of colloidal and polymer suspensions[13, 14, 20–22]. The method is also known as "Real-coded Lattice Gas"[20] or as "multi-particle-collision dynamics" (MPCD)[22] and is based on coarse-grained fluid particles with continuous positions and velocities. A streaming step and an interaction step are performed alternately. In the streaming step, each particle i is moved according to $\vec{r}_i(t+\tau) = \vec{r}_i(t) + \tau\,\vec{v}_i(t)$, where $\vec{r}_i(t)$ denotes the position of the particle i at time t and τ is the time step. In the interaction step fluid particles are sorted into cubic cells of a regular lattice and only the particles within the same cell interact according to an artifical collision rule which conserved energy and momentum. First, for each independent cell j the mean velocity $\vec{u}_j(t') = \frac{1}{N_j(t')}\sum_{i=1}^{N_j(t')}\vec{v}_i(t)$ is calculated. $N_j(t')$ is the number of fluid particles contained in cell j at time $t' = t+\tau$. Then, the velocities of each fluid particle are rotated according to

$$\vec{v}_i(t+\tau) = \vec{u}_j(t') + \vec{\Omega}_j(t')\cdot[\vec{v}_i(t) - \vec{u}_j(t')]. \quad (3)$$

$\vec{\Omega}_j(t')$ is a rotation matrix, which is independently chosen at random for each time step and cell. Rotations are about one coordinate axes by a fixed angle $\pm\alpha$. To couple colloidal particles and the fluid, the particles are sorted into SRD cells and their velocities are included in the rotation step. The masses of colloidal and fluid particles are used as a weight factor for the mean velocity

$$\vec{u}_j(t') = \frac{1}{M_j(t')}\sum_{i=1}^{N_j(t')}\vec{v}_i(t)m_i, \quad (4)$$

$$\text{with} \qquad M_j(t') = \sum_{i=1}^{N_j(t')} m_i. \quad (5)$$

$N_j(t')$ is the total number of all colloidal and fluid particles in the cell. m_i is the mass of particle i and $M_j(t')$ gives the total mass contained in cell j at time $t' = t+\tau$. We apply shear by explicitly setting the mean velocity $\vec{u}_j$ to the shear velocity in the cells close to the border of the system. A thermostat removes the energy introduced to the system by the shear force.

One simulation run takes between one and seven days on a 3GHz Pentium CPU. In order to be able to gather statistics as well as to minimize finite size effects, we parallelized our code. While MD codes have been parallelized by many groups, only few parallel implementations of a coupled MD and SRD program exist. This is in contrast to the number of parallel implementations of other mesoscopic simulation methods like for example the lattice Boltzmann method. A possible explanation is that SRD is a more recent and so far not as widely used algorithm causing the parallelization to be a more challenging task.

We study systems [23] containing a volume concentration of 5% of colloidal particles (=1320 MD particles), a shear rate of $\dot{\gamma} = 20/s$, ionic strengths I= 3mmol/l and 7mmol/l, and pH = 6 and 7. To demonstrate the effect of clustering, in fig, (1) snapshots from a typical simulation of a $8.88\mu m^3$ system with periodic boundaries at I = 7mmol/l and pH = 6 at different times are shown. While at the beginning of the simulation (a), freely moving particles can be observed, small clusters appear after $t = 0.26$s (b). After $t = 1.06$s, all particles are contained within three individual clusters (c) and after $t = 4.22$s only one single cluster is left in the system. For an investigation of

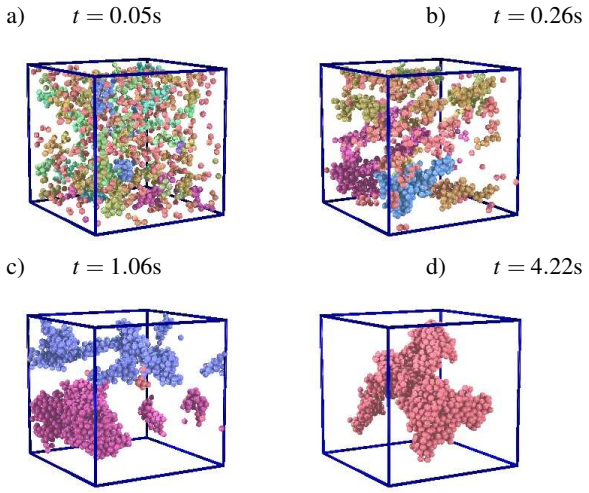

FIG. 1: Snapshots of a simulation of an $8.88\mu^3$ system, filled with $\Phi = 5\%$ MD particles of diameter $d = 0.37\mu$ under shear with $\dot{\gamma} = 20/s$.

the formation and movement of clusters, substantially larger systems are needed. Therefore, we scaled up the simulation volume to $17.76\mu^3$ containing 10560 MD particles and $1.3{\cdot}10^7$ fluid particles. Due to the computational demands of the fluid solver, a single simulation of 5s real time requires about 5000 CPU hours on 32 CPUs of an IBM p690 system.

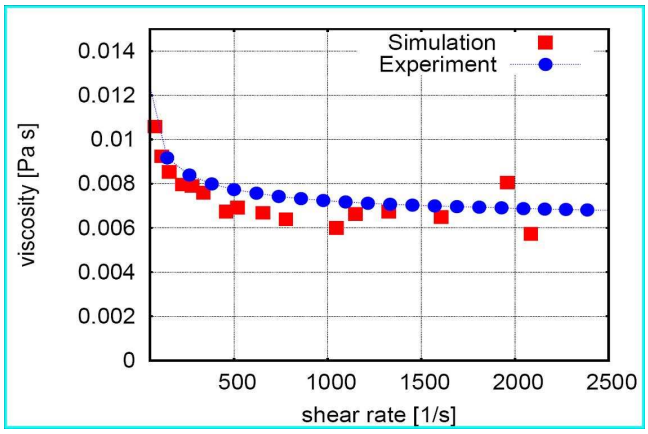

FIG. 2: Viscosity as function of shear velocity.

Using this algorithm we can calculate the viscosity and obtain the result shown in Fig. 2. We compare this with experimental data obtained by Reinshagen in Karlsruhe for aluminum oxyde beads in water at pH = 6 under shear [14]. We see that the agreement is good and that the numerical data show much more scatter that the experimental one because the simulated system is much smaller. Another reason for discrepancy is the insecurity in the experimental determination of the ζ-potential. Clearly the system exhibits shear softening, i.e. the viscosity decreases with the shear rate. This is very typical for dense colloids.

Summarizing, the presented combination of MD and SRD has turned out to be very accurate to simulate colloids of nano-sized particles where van der Waals and electrostatic forces compete with thermal motion. Besides the cluster formation and the rheology presented here we have also measured correlations functions and structure factors [12].

III. THE VELOCITY DISTRIBUTION

The probability distribution function of particle velocities $P(v)$ can be of use for a better understanding of colloids. Naively, one might expect $P(v)$ to be of similar shape as for an ideal gas, i.e., like a Maxwellian. However, it has been found by numerous authors that the probability of high velocities is substantially larger than predicted by a Gaussian shaped distribution function [24, 25]. Non-Gaussian distributions are well known from other fields of physics like granular media [26–28], astrophysics [29], flow in porous media [30], turbulence [31], bubble rafts [32] or glass forming colloids [33]. Experimentally, Rouyer et al. [34] studied quasi 2D hard-sphere suspensions and found a stretched exponential form of $P(v)$ with concentration dependent exponents between 1 and 2 corresponding to purely exponential distributions for high concentrations and a Gaussian for small particle counts. These experimental results are in contrast to theoretical predictions of a transition from exponential to Gaussian with increasing volume concentration [24, 25]. However, both experimental and theoretically studied systems are not able to obtain valuable statistics over more than 2-4 decades. If one does not have enough data for high quality PDFs, a final answer on the nature of the function cannot be given since for high velocities the variation of the data points is too large. Indeed, we have found that even stretched exponentials can fit PDFs with purely exponential tails and Gaussian centers if only 2-4 decades of probability are covered [35]. But as soon as one adds more data points, the exponential nature of the tails becomes more distinct and fitting the whole PDF with a single stretched exponential function becomes impossible.

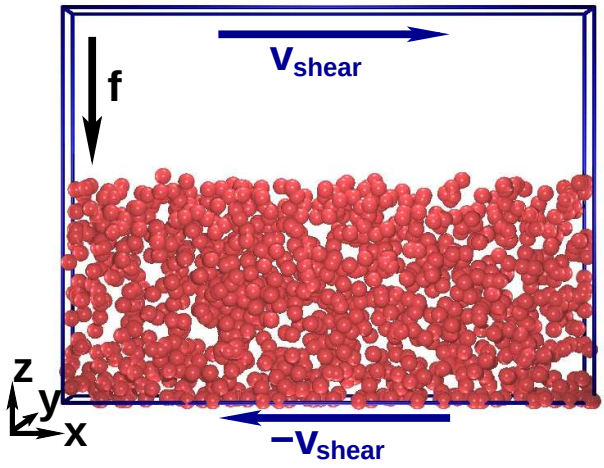

FIG. 3: Sketch of the simulation setup.

In this section we follow our work being reported on in [35]. We overcome the limitations of previous works by presenting PDFs consisting of up to 10^{10} measurements of particle displacements each [35]. Our data does not show any deviations from purely exponential tails over six to eight decades of probability. Using a single-particle theory we can analytically confirm this finding. We show that for constant volume concentration ϕ, $P(v_z)$ scales linearly with the shear rate, volume concentration and viscosity. The system under consideration is a three-dimensional Couette setup as shown in Fig. 3. At top and bottom closed sheared walls are applied and the shear rate is $\dot{\gamma} = 2v_{\text{shear}}/N_z$, with N_z being the distance between the shear planes. All other boundaries are periodic. We consider 384 up to 1728 initially randomly placed suspended particles of equal radius corresponding to a particle volume concentration ϕ between 6.8% and 30.7%. A body force f can be added to mimic gravity.

We apply a hybrid method composed of a lattice-Boltzmann solver (LB) for the fluid solvent and a molecular dynamics (MD) algorithm for the motion of suspended particles. With appropriate boundary conditions being imposed at solid/fluid interfaces, colloidal suspensions can be modeled. This approach and recent additions for the calculation of lubrication forces and stability improvements of the MD were originally introduced by A.J.C. Ladd and coworkers [36–39]. The algorithm has been applied by numerous groups and is well established in the literature [36–41]. For our simulations we found a particle radius of a=1.25 lattice sites being sufficient since for larger particles $P(v_z)$ does not change significantly anymore, but the computational effort increases substantially. The simulation volume has dimensions $64a \times 8a \times 48a$ and the shear rate $\dot{\gamma}$ is varied between $2.3 \cdot 10^{-4}$ and $1 \cdot 10^{-3}$ (in lattice units). The fluid density is kept constant and if not specified otherwise the kinematic viscosity is set to $\nu = 0.05$.

One simulation runs for 6.25 million lattice Boltzmann time steps, where during the last 5 million time steps the z component of the velocity of every individual particle is gathered in a histogram in order to obtain $P(v_z)$. Up to 10^{10} data points per histogram allow us to obtain good statistics over six orders of magnitude. All distributions are normalized such that $\int \mathrm{d}v_z P(v_z) = 1$ and $\int \mathrm{d}v_z v_z^2 P(v_z) = 1$.

The theoretical model [35] is based on the balance between viscous dissipation and shear forcing in steady state. The forcing is modeled as uncorrelated white noise ($\langle \xi_j \rangle = 0$, $\langle \xi_i(t)\xi_j(t')\rangle = 2D\delta_{ij}\delta(t-t')$). velocities change as $\frac{dv_j}{dt}|_{\text{heat}} = \xi_j$. Due to the viscous fluid, particles slow down. The change in the velocity is $dv/dt = -\beta v$, so in accordance with the traditional drag law the velocity decays exponentially in the absence of forcing $v = v_0 e^{-\beta t}$. We model this by reducing each time unit the velocity by a factor $\eta = e^{-\beta}$ as $v \to \eta v$. In a sheared fluid, there is a well defined time scale for re-encounters with the boundary, setting the time scale for the damping process. This process was used by van Zon et al. to model forced granular media [42, 43]. The velocity distribution obeys the linear equation

$$\frac{\partial P(v)}{\partial t} = D\frac{\partial^2 P(v)}{\partial^2 v} + \frac{1}{\eta} P\left(\frac{v}{\eta}\right) - P(v). \qquad (6)$$

Here, no explicit interactions between particles are considered. Instead, a particle undergoes diffusion as influenced by all other particles. This effect is modeled by the first term on the right hand side. The next two terms describe gain and loss due to the damping. In steady state the left hand side of Eq. 6 vanishes. We note that the shape of $P(v)$ is independent of the diffusion constant. Indeed, by making the scaling $v \to v/\sqrt{D}$ we can eliminate D and assume without loss of generality that $D = 1$. The shape of the distribution depends on the dissipation parameter η alone. In the weak drag limit, $\eta \to 1$, the exponential decay holds only for sufficiently large velocities and there is a cross-over between a Maxwellian behavior and an exponential one,

$$P(v) \sim \begin{cases} \exp\left(-\frac{\varepsilon v^2}{2}\right) & v \ll \varepsilon^{-1}, \\ \exp\left(\frac{\pi^2}{12\varepsilon} - |v|\right) & v \gg \varepsilon^{-1}, \end{cases} \qquad (7)$$

where $\varepsilon = 1 - \eta$. The two expressions match, $P(v) \sim \exp\left(-\varepsilon^{-1}\right)$ at the crossover velocity $v \approx \varepsilon^{-1}$. The Maxwellian behavior directly follows from the moments. Interestingly, the crossover to a non-Maxwellian does not affect the leading behavior of the moments.

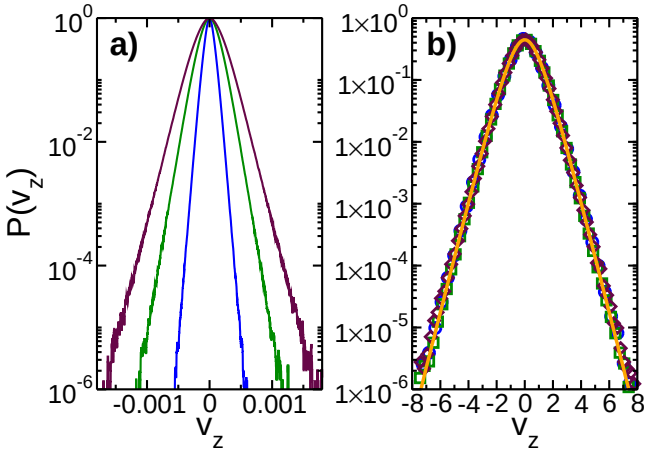

FIG. 4: Probability distribution function of v_z for $f = 0.72 \cdot 10^{-4}$ corresponding to a Stokes velocity of v_s=1.4 $\cdot 10^{-3}$, $\phi = 13.6\%$ and different shear rates $3.3 \cdot 10^{-4}$, $6.7 \cdot 10^{-4}$, and $1 \cdot 10^{-3}$. The left figure shows the unscaled data, where higher $\dot{\gamma}$ relate to wider $P(v_z)$. The right figure shows a collapse of the data obtained by normalising as described in the text. The full line is the steady state solution of Eq. 6 ($\eta = 0.73$) [35].

As a summary, the theory predicts the non-equilibrium shape of the PDF as an interplay between energy being injected by a diffusive thermostat and dissipation due to the drag of the fluid. The theoretical results shown later are given by a Monte Carlo solution of the steady state case of Eq. 6. Here, N particles are characterized by a velocity v_i. The velocities change through two independent processes: damping and random forcing. In the damping process, the velocity is reduced by a fixed factor $v_i \to \eta v_i$. In the forcing process, the particle velocity changes by a random increment $v_i \to v_i + \xi$ where ξ has zero mean and a unit variance. The steady-state distribu-

tions were obtained using over 10^{10} points from simulations with 10^8 particles.

Let us first consider suspensions with constant volume concentration and various shear rates under the influence of a body force f. The dependence of $P(v_z)$ on the shear rate for three representative $\dot{\gamma}$ is depicted in Fig. 4a. Distributions in other directions are essentially identical if one deducts the shear velocity and are therefore not shown. $P(v_z)$ is symmetric and $\langle v_z \rangle = 0$ for all cases considered in this proceedings paper. As shown in Fig. 4b, the not normalized distributions widen for higher shear rates. However, a very good scaling is observed: all normalized curves collapse onto a single one. The influence of $\dot{\gamma}$ on the RMS velocity $v_z^{\mathrm{RMS}} = \sqrt{\langle v_z^2 \rangle}$ follows a linear dependence as expected from the theory: the shear rate only sets a scale for the velocity.

To obtain an insight into the properties of $P(v_z)$, we compute the cumulant κ from our data and find that for all simulation parameters studied in this letter it varies between 3.8 and 4.6. Knowing κ, we can compute $\eta = \sqrt{6/\kappa - 1}$. Due to the large number of data points in our histograms, we calculate κ for periods of 1 million time steps each and then compute the arithmetic average of the last 5 million time steps of a simulation run. We find that κ varies by up to 10% within a single simulation which is of the same order as the difference of the individual PDFs in Fig. 4b. Thus, we average the different curves as well in order to obtain a value for the cumulant to be utilized for the Monte Carlo solution of the steady state case of Eq. 6. For the collapse in Fig. 4b we get $\eta = 0.73$. As demonstrated in the figure, the solid line given by the theory and the simulation data show an excellent agreement over the full range of six orders of magnitude of probability.

We consider next neutrally-buoyant suspended hard-spheres under shear. The shear rate is kept fixed and the particle volume concentration is varied between $\phi = 6.8\%$ and 30.7%. Due to hydrodynamic interactions, the particles tend to move to the center of the system, i.e., to an area where the shear is low creating a depleted region close to the sheared walls. The corresponding normalized $P(v_z)$ are presented in Fig. 5a. As depicted in the figure, all PDFs except for the lowest particle concentration $\phi = 6.8\%$ (circles) collapse onto a single curve. At very low concentrations, the tails of $P(v_z)$ are still not fully converged due to the limited number of particle-particle interactions taking place within the simulation time frame. Again, the full line in Fig. 5a is given by the steady state solution of Eq. 6 with $\eta = 0.69$ being obtained from the fourth moment of $P(v_z)$. As before, a very good agreement between simulation and theory is observed. We study the dependence of v_z^{RMS} on ϕ. For concentrations of at least $\phi = 13.6\%$ $v_z^{\mathrm{RMS}}(\phi)$ can be fitted by a line with slope $1.8 \cdot 10^{-4}$.

By keeping all simulation parameters except the kinematic viscosity ν constant, the dependence of ν on $P(v_z)$ can be studied. We find that the probability distribution functions are independent of the viscosity. Thus, the steady state curve obtained for different volume concentrations is identical to the one for different ν as shown in Fig. 5b. It would be of interest to study the influence of the body force f on the shape of the probability distribution. However, f and the shear forces are in a subtle interplay since the height of the steady state sediment depends on both parameters and thus influences the local particle volume concentration. To investigate this behavior is beyond our scope.

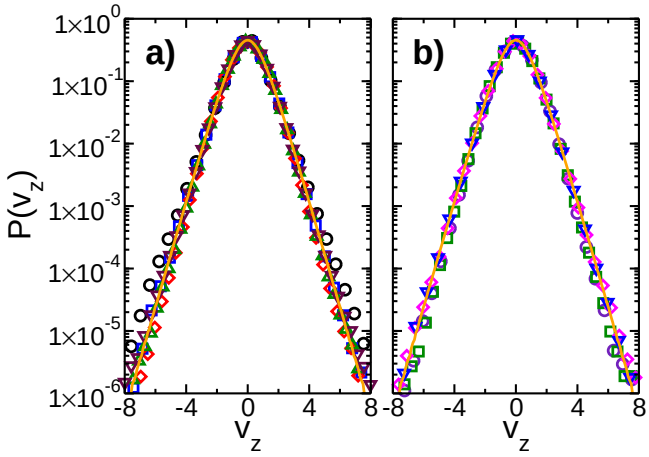

FIG. 5: $P(v_z)$ for $f = 0$, $\dot{\gamma} = 6.7 \cdot 10^{-4}$ and $\phi = 6.8\%, 13.6\%, 20.5\%, 23.9\%$, and 27.3% **(a)**. In Fig. **b)**, ϕ is kept at 13.6% and the kinematic viscosity is set to $\nu = 0.017$, 0.05, and 0.1. In both figures, all data sets collapse onto a single curve and the lines are given by the theory with $\eta = 0.69$ [35].

We conclude that the non-equilibrium velocity distributions reported here are a consequence of the irreversible nature of the driving process. On average, particles gain energy by one mechanism but lose energy by another mechanism and unlike in an ideal gas, these two mechanisms are not interchangeable. In other words, one cannot reverse the arrow of time and observe the same behavior. Our theoretical model captures this irreversibility through the competition between two non-equivalent driving mechanisms: energy dissipation through a multiplicative process and energy injection through an ordinary additive diffusive thermostat. The theory describes all aspects of the distribution as demonstrated by an excellent agreement with the results obtained from our coupled lattice Boltzmann and molecular dynamics simulations of sheared hard-sphere suspensions: the particle velocity distribution functions $P(v_z)$ exhibit a Gaussian core and exponential tails over at least six orders of magnitude of probability. Interestingly, particle interactions in moderately dense suspensions can be well represented by a white noise. We also note that the complete shape of the distribution function can be characterized by a single parameter, the normalized fourth moment.

IV. CONCLUSION

In this proceedings we have demonstrated an efficient way to simulate dense colloids by combining MD with either SRD or lattice Boltmann. We applied the first algorithm to data obtained from large scale simulations of colloidal suspensions in the clustering regime and found the shear softening of the viscosity in good agreement with experiments. Further, by applying the latter method, we confirmed that $P(v_z)$ scales lin-

early with the particle volume concentration as well as the shear rate and is independent of the solvent's viscosity. While different authors report on transitions between Gaussian and (stretched) exponential tails [24, 25, 34], we have shown that such findings are due to insufficient statistics and that there is no such transition.

Acknowledgments

We thank A.J.C. Ladd for providing his code and G. Gudehus, M. Külzer, L. Harnau, M. Bier, J. Reinshagen, and A. Coniglio for valuable collaboration. This work was supported by DFG, US-DOE and the German-Israeli Foundation (GIF). JH acknowledges a scholarship by the "Landesstiftung Baden-Württemberg" and HJH thanks the Max Planck prize. The computations were performed on the IBM p690 cluster at Forschungszentrum Jülich, Germany.

[1] W. B. Russel, D. A. Saville, and W. Schowalter, *Colloidal Dispersions*, Cambridge University Press, 1995.
[2] R. J. Hunter. *Foundations of colloid science*. Oxford University Press, Oxford, 2001.
[3] S. Richter and G. Huber, *Granular Matter*, **5**, 121 (2003).
[4] S. Richter. *Mechanical Behavior of Fine-grained Model Material During Cyclic Shearing*. PhD thesis, University of Karlsruhe, Germany, 2006.
[5] R. Tuinier, G. A. Vliegenthart, and H. N. W. Lekkerkerker, J. Chem. Phys. **113**, 10768 (2000).
[6] D. Rudhardt, C. Bechinger, and P. Leiderer, Phys. Rev. Lett. **81**, 1330 (1998).
[7] B. V. R. Tata, E. Yamahara, P. V. Rajamani, and N. Ise, Phys. Rev. Lett. **78**(13), 2660 (1997).
[8] P. Linse and V. Lobaskin, Phys. Rev. Lett. **83**(20), 4208 (1999).
[9] M. Hütter. *Brownian Dynamics Simulation of Stable and of Coagulating Colloids in Aqueous Suspension*. PhD thesis, Swiss Federal Institute of Technology Zurich, 1999.
[10] G. Wang, P. Sarkar, and P. S. Nicholson, J. Am. Ceram. Soc. **82**(4), 849 (1999).
[11] M. Hütter, J. Colloid Interface Sci. **231**, 337 (2000).
[12] M. Hecht, J. Harting, and H. J. Herrmann, Phys. Rev. E, **75**, 051404 (2007).
[13] M. Hecht, J. Harting, T. Ihle, and H. J. Herrmann, Phys. Rev. E, **72**, 011408 (2005).
[14] M. Hecht, J. Harting, M. Bier, J. Reinshagen, and H. J. Herrmann, Phys. Rev. E, **74**, 021403 (2006).
[15] E. J. W. Vervey and J. T. G. Overbeek, *Theory of the Stability of Lyophobic Colloids*. Elsevier, Amsterdam, 1948.
[16] B. V. Derjaguin and L. D. Landau, Acta Phsicochimica USSR, **14**, 633 (1941).
[17] A. Malevanets and R. Kapral, J. Chem. Phys., **110**, 8605 (1999).
[18] A. Malevanets and R. Kapral, J. Chem. Phys., **112**, 7260 (2000).
[19] M. P. Allen and D. J. Tildesley, *Computer simulation of liquids*. Oxford Science Publications. Clarendon Press, Oxford, 1987.
[20] Y. Inoue, Y. Chen, and H. Ohashi, J. Stat. Phys., **107**(1), 85 (2002).
[21] J. T. Padding and A. A. Louis, Phys. Rev. Lett., **93**, 220601 (2004).
[22] M. Ripoll, K. Mussawisade, R. G. Winkler, and G. Gompper, Phys. Rev. E, **72**, 016701 (2005).
[23] M. Hecht, J. Harting, and H. J. Herrmann, Int. J. Mod. Phys. C, **18**, 501 (2007).
[24] G. Drazer, J. Koplik, B. Khusid, and A. Acrivos, J. Fluid Mech., **460**, 307 (2002).
[25] M. Abbas, E. Climent, O. Simonin, and M. Maxey, Phys. Fluids, **18**, 121504 (2006).
[26] K. Kohlstedt, A. Snezhko, M. V. Sapozhnikov, I. S. Aranson, J. S. Olafsen, and E. Ben-Naim, Phys. Rev. Lett., **95**, 068001 (2005).
[27] R. Cafiero, S. Luding, and H. J. Herrmann, Phys. Rev. Lett., **84**, 6014 (2000).
[28] D. J. Bray, M. R. Swift, and P. J. King, Phys. Rev. E, **75**, 062301 (2007).
[29] M. S. Miesch and J. M. Scalo, Astrophys. J., **450**, L27 (1995).
[30] J. F. Olson and D. H. Rothman, J. Fluid Mech., **341**, 343 (1997).
[31] B. I. Shraiman and E. D. Siggia, Nature, **405**, 639 (2000).
[32] Y. Wang, K. Krishan, and M. Dennin, Phys. Rev. Lett., **98**, 220602 (2007).
[33] E. R. Weeks, J. C. Crocker, A. C. Levitt, A. Schofield, and D. A. Weitz, Science, **287**, 627 (2000).
[34] F. Rouyer, J. Martin, and D. Salin, Phys. Rev. Lett., **83:**, 1058 (1999).
[35] J.Harting, H.J. Herrmann and E. Ben-Naim, *arXiv.0707.4356* (2007).
[36] A. J. C. Ladd, J. Fluid Mech., **271**, 285 (1994).
[37] A. J. C. Ladd, J. Fluid Mech., **271**, 311 (1994).
[38] N. Q. Nguyen and A. J. C. Ladd, Phys. Rev. E, **66**, 046708 (2002).
[39] A. J. C. Ladd and R. Verberg, J. Stat. Phys., **104**, 1191 (2001).
[40] N. Q. Nguyen and A. J. C. Ladd, Phys. Rev. E, **69**, 050401(R) (2004).
[41] A. Komnik, J. Harting, and H. J. Herrmann, J. Stat. Mech: Theor. Exp., P12003 (2004).
[42] J. S. van Zon, J. Kreft, D. I. Goldman, D. Miracle, J. B. Swift, and H. L. Swinney, Phys. Rev. E, **70**, 040301(R) (2004).
[43] H. Larralde, J. Phys. C., **37**, 3759 (2004).